

Špiro Ivošević

E-mail: spiroi@ucg.ac.me

University of Montenegro, Maritime Faculty Kotor

Dobrota 36, 85330 Kotor, Montenegro

Peter Majerič

E-mail: peter.majeric@um.si

University of Maribor, Mechanical Engineering Faculty

Smetanova ulica 17, 2000 Maribor, Slovenia

Miroslav Vukičević

E-mail: miroslav.vukicevic@ucg.ac.me

University of Montenegro, Maritime Faculty Kotor

Dobrota 36, 85330 Kotor, Montenegro

Rebeka Rudolf

E-mail: rebeka.rudolf@um.si

University of Maribor, Mechanical Engineering Faculty

Smetanova ulica 17, 2000 Maribor, Slovenia

A Study of the Possible Use of Materials With Shape Memory Effect in Shipbuilding

Abstract

The article presents a study of the possible use of materials with Shape Memory Effect (SME) in shipbuilding, which have two special abilities of transformation and changing shape with changing of temperature or deformation. Among the most well-known SME materials, our study focuses on Ni-Ti and Cu- based alloys. An example of the existing fabrication presents casting of Ni-Ti in the form of a disk, and a new approach – continuous casting of Ni-Ti and CuAlNi alloys in the form of rods. In the article some results are shown of characterisation of microstructure and the basic properties. This was done in accordance with the fact that such scientific approach could define the starting point for further identification of the functional characteristics of these alloys by knowing the their chemical content and microstructure. Numerous studies are being carried out today in order to find the optimal functional characteristics of SME alloys. All of this is aimed at optimising the fabrication of these alloys, with the achievement of suitable properties for application in shipbuilding.

Keywords: shipbuilding, Shape Memory Effect, alloys, microstructure, mechanical properties, corrosion, testing

1. Introduction

Since the discovery of the Shape Memory Effects (SME) in 1932 until the present day, numerous researches have been aimed at examining different alloys that undergo thermoplastic martensite transformation [1, 2]. To date, a research of many alloys with SME has been considered for possible use. Today, the most important Shape Memory Alloys (SMA) are based on Ni, Cu and Al [2]. Research of SMA in different branches of industry led to discoveries of other unique phenomena, such as Super Elasticity (SE) and their ability for doing work or damping vibration (so-called high damping) [3]. By testing of material on the basis of Ni-Ti with SME during the 1960s and 1970s of the last century, the production of different products in ships and submarines was initiated in the U.S. Navy, Aeronautics, the Rail road and Maritime sectors, the Automotive sector, Telecommunications, Robotics, and the medical industry. The research was focused in terms of discovering the scope of SMAs, and their features for possible use in the shipbuilding industry, where the combination of high strength and ductility and corrosion resistance is required. These SMAs have the ability to change their shape, position, stiffness, natural frequency and other mechanical characteristics when expanding to temperature.

This paper presents the basic information of SMAs which were produced by the conventional approach (casting) in comparison with the technological procedure Continuous Casting (CC). SMAs were produced in the shape of discs through casting and rods by CC. The samples of both SMAs were prepared for metallographic testing, in order to perform microstructure analysis and identification of some properties. The discussion is focused on the prediction if newly developed SMAs could be used for shipbuilding under certain conditions.

2. About different types of SMA

SMAs are characterised primarily by their capacity to restore their original dimensional integrity (pre-deformed shape and size) after undergoing substantial deformation when heated to a certain temperature [4]. This temperature induced strain recovery and other elasticity variants exhibited by SMAs, make them suitable for application in various industrial branches. In Figure 1 it is possible to see the typical stress limits and recoverable strain of SMAs compared to other engineering materials [5].

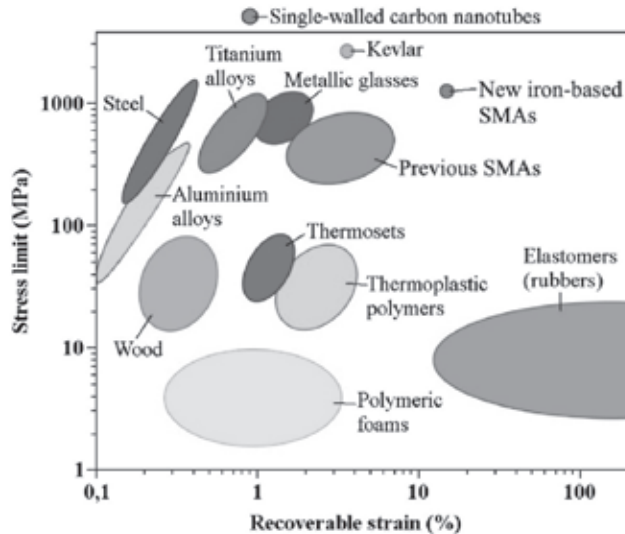


Figure 1: Typical stress limits and recoverable strain of SMAs compared with other engineering materials [8]

During recent research of SMAs many types of alloys appeared, and they were made on the basis of Au, Al, Cu, Ni, Ti. Etc. Today, the most known are binary alloys: Ag–Cd, Au–Cd, Cu–Sn, Cu–Zn, In–Ti, Ni–Al, Ni–Ti, Mn–Cu, Fe–Pt and ternary Cu–Al–Ni, Cu–Zn–X (X = Al, Si, Sn, Ga), Fe–Mn–Si [3]. Up to now, the most important SMA application can be attributed to Ni–Ti, Cu–Al–Ni and Cu–Zn–Al, as well as Fe-based alloys. Detailed analysis shows that Ni–Ti are, up to now, the most functional, successful and commercially utilised SMAs, Cu alloy systems are reported to exhibit superior shape memory functionality and have processing cost advantages. On the other hand, Fe-based SMAs have good workability, and can be produced via commercial steel making processes [6, 7]. Ni–Ti SMAs have the greatest application in commercial purposes of different industry branches, such as biomedical (blood clot filters, orthodontic corrections), while Cu- and Fe- are aimed mainly for industrial use (fluid connectors and couplings), thermal actuators (fire alarms, fire safety valves) and other domestic applications (eye glass frames, bra under-wires) [8].

Transformation temperature range, Hysteresis, and Maximum recovery strain are the SMA key characteristics, which are presented in Table 1, with conventional chemical composition and the type of martensite for representative SMAs.

Table 1: Main characteristics of some SMAs [9, 2]

SMAs	Martensite	Trans.range (°C)	Hysteresis (°C)	Max. Rec. Strain (%)
Ti-Ni	Monoclinic B19	-100 to 100	~ 30	6 - 8
Ti-Ni + Ti-Ni-Fe	Trigonal R	-20 to 70	2 - 3	1
Ti-Ni-Cu	Orthorhombic B19	30 to 80	10 – 15	5 - 6
Ti-Ni-Nb	Monoclinic B19'	-150 to 70	70 – 120	8
Ti-Ni-Pd	R+B19'+B19	0 to 250	30 – 50	3 – 4
Cu-Zn-Al	Monoclinic 6M	-200 to 100	10 - 30	6
Cu-Al-Ni	Orthorhombic η'	-150 to 100	~ 35	8 ($\rightarrow\beta'$)
Cu-Al-Ni	Monoclinic β'	50 to 200	~ 10	➤ 10 (SX)

Nickel and copper were two of the most useful elements in the building of SMAs. Due to their different physical and chemical properties, which influences the final SMAs' microstructure, the properties of NiTi and CuZnAl alloys are fairly different, as is shown in Table 2. Because Ni-Ti alloys have better physical and thermo-mechanical characteristics than CuZnAl (higher strength, larger recoverable strain, better corrosion resistance, higher reliability), they are more useful for different applications in industry [2].

Table 2: Comparison of NiTi/CuZnAl alloys [10]

Process factors	Ni-Ti	Cu-Zn-Al
Recover strain	max S%	max 4%
Recover stress	max 400 Mpa	max 200 Mpa
Number of cycles	10^5 ($\epsilon = 0.02$) 10^7 ($\epsilon = 0.05$)	10^2 ($\epsilon = 0.02$) 10^5 ($\epsilon = 0.05$)
Corrosion resistance	good	Problematic, especially stress, corrosion cracking
Workability SM processing	Poor comparatively easy	Fair Fairly difficult

Cu- based SMAs can be strained up to 10% and then converted to their primary shape [11]. These SMAs are available for the transformation temperature range between -200 and +200 (°C). Typical SMAs are Cu-Zn-Al and Cu-Al-Ni, which are the most

available on the market, and can be used for different commercial applications. They are easy to produce/fabricate and, consequently, in comparison to Ni-Ti, their production process is significantly cheaper.

3. Production of testing SMA materials

NiTi and CuAlNi can be produced by different production techniques. One of the main problems of SMAs is the possibility for further plastic deformation, especially cold drawing, due to the large grain size and existence of different brittle intermetallic phases. In order to overcome these two problems, a new processing technique was used, CC [12,13,14,15]. With the CC processing technique, the cast product can have a significantly smaller cross-section (as close as possible to the final dimension of the product), thus avoiding further plastic processing. To our knowledge, the CC technique has, to date, never been used, or only to a limited extent, for the production of SMA rods. The experimental device at the Faculty of Mechanical Engineering, Maribor, Slovenia, consists of a vacuum induction melting furnace and a vertical continuous caster. The fact is that, in recent years, several very successful research stories have been accomplished with this experimental set up (research CC of small dimension rods of gold and silver-based alloys). CC is not yet well studied in the frame of SMAs, due to the many technical limitations (high reactivity of Ti, high viscosity of Ti in liquid form, problems with stirring of the melt).

For the first time, rods of SMAs (Ni-Ti and CuAlNi), with diameter of around 13 mm, have been cast. Experiments with CC are carried out on the vertical CC device. An adequate quantity of each component (Cu, Al, Ni, Ti) with a common weight around 20 kg, was placed into the induction furnace in the required proportions for the preparation of each alloy separately. A vacuum (10^{-2} mbar) was achieved in the furnace. After heating to the temperature of casting (about 50°C above the temperature of melting for NiTi = 1350°C and for CuAlNi = 1100°C), the continuous process started with SMA casting (drawing) of a rod at overpressure of Ar (5.1). Casting of the rods was carried out in the regime of (stop/go), with different periods of stopping and going. The solidified rods ran out from the CC device through a nozzle, where the melting/cooling conditions affected the final microstructure of both rods strongly.

4. Preparation of samples and methods of testing

4.1. Preparing of samples

a) Cutting of disc and rods

The initial material Ni-Ti (in two states: NiTi 1 – as cast, NiTi 2 CC -) and CuAlNi 3 - CC - were cut by electro-erosion to the selected dimensions for preparing suitable samples in 27 pieces for corresponding corrosion tests in the sea - (nine pieces of each

type of SMAs - as shown in Figs. 2a - 2c. Samples made from NiTi were in the form of a disc (Figure 2a), while the rod of NiTi had a diameter of 12 mm (Figure 2b) and the rod of CuAlNi a diameter of 7 mm (Figure 2c). All test samples were ground after electro-erosion to remove erosion residues and impurities.

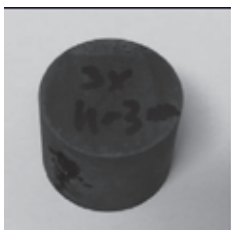


Figure 2a: NiTi 1 as cast

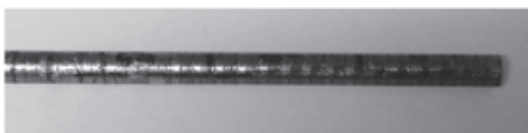


Figure 2b: NiTi 2 CC (diameter - $2r=7\text{mm}$)



Figure 2c: CuAlNi 3 (diameter - $2r=7\text{mm}$)

b) Metallographic sample preparation

The samples were then mounted in a hot-mounting mass and ground with abrasive paper in grades of 180-4000 on the grinding/polishing machines BUEHLER Automet 250 and EcoMet 250 (Figs. 3a and 3b). The samples were polished with a napless cloth and polishing suspension with Al_2O_3 with the size of $1\ \mu\text{m}$. After polishing, samples were cleaned by ultrasound. This process was followed by etching, in order to reveal the microstructure of the samples.



Figure 3a: BUEHLER Automet 250



Figure 3b: EcoMet 250

The following chemicals were used for etching:

NiTi 1 – 3 ml HF, 6 ml HNO₃, 100 ml H₂ – etching time 105 s,

NiTi 2 – 3 ml HF, 6 ml HNO₃, 100 ml H₂ – etching time 120 s,

CuAlNi - 5g FeCl₃, 10 ml HNO₃, 100ml H₂O – etching time 30 s.

4.2. Microstructure observation

a) Optical microstructure

Light microscopy was used in order to investigate the surface of materials and get a clear impression of the entire investigated surface of the sample. The light microscope consists of a light source, glass lenses and a prism, semipermeable mirrors, an ocular lens (which represents the first part of the lens system through which the light travels), an objective lens (which focuses the light on the ocular lens), and a filter system. The light beam travels from the light source through the lens system, which directs the jet parallel to the optical axis. With an aperture shutter we regulate the amount of light for illumination, in order to achieve optimum sharpness and contrast of the image. The field of vision is increased or decreased with a field shutter. The objective lens consists of a lens system that increases the image of the investigated surface from 5- to 100-times. The prism redirects the light into the ocular lens, which increases the image further by 5-10-times. This picture can then be viewed with the naked eye and recorded with the camera on a computer.

The microstructure of the test samples was examined on the Nikon EPIPHOT 300 light microscope (Figure 4). The sample examination on the OM Nikon Epiphot 300 was done by illuminating the sample from below. Magnifications are possible from 50 - 1000x, so microstructures can be examined on the 20 μ m scale. Image processing with OM was done using the Analysis programme, which allows measurements of lengths, determining the surface area and size of grains, determining the content of two or more phases, and content of inclusions.



Figure 4: Nikon EPIPHOT 300

b) Micro hardness measurement of test samples

The hardness is the resistance of the material against a foreign body's invasion through its surface. For the Vickers method, the imprint is a four-sided diamond pyramid with a peak angle of 136° . With constant force, we imprint the impregnating body on the surface of the specimen, and cause local plastic deformation of the material. After the load is released, the length of the diagonal of the imprint is measured (Figure 5), then the hardness is calculated according to the corresponding equation:

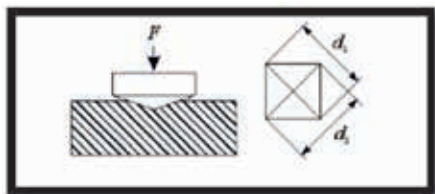


Figure 5: Micro hardness measurement and imprint display

$$\text{(number of } d_1 \text{ units} \times \text{value of } d_1) + \text{(number of } d_2 \text{ units} \times \text{value of } d_2). \quad (1)$$

The micro hardness HV5 was measured on the ZWICK 3212 (Figure 6.a), and the HV50 on the WPN HPO 250 (Figure 6.b).

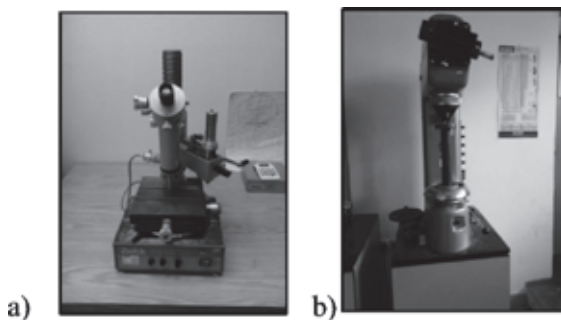


Figure 6: a) Micro hardness ZWICK 3212, b) Micro Hardness WPN HPO 250

The Vickers microhardness device ZWICK 3212 provides a sample load of 0.098 N (HV 0.01) to 49.02 N (HV50). Higher loads are possible on the WPM HPO-250 hardness measuring device,. The meter was calibrated in January 2019 according to the requirements of SIST EN ISO 6507-2. The calibration was performed by direct and indirect methods, and an accredited Certificate was issued.

c) ICP Analysis

Inductively Coupled Plasma Analyses (ICP Analysis), was performed to identify and measure a range of the chemical elements necessary for the analysis of metal

samples. ICP-AES Analysis and ICP-MS Analysis test methods can be performed on solid or liquid samples. ICP metal analysis can determine up to 70 elements. Trace unknowns can be detected and identified. In addition, ICP analysis can reveal several non-metals.

ICP MS Analysis, Inductively Coupled Plasma Mass Spectrometry (ICP-MS) or ICP Mass Spectrometry is highly sensitive, and capable of multi-element trace analysis and ultra trace analysis, often at the parts-per-trillion level. Testing for trace elements can be performed on a range of materials from super alloys to high purity materials.

d) XRF Analysis

XRF is a non-destructive analytical technique used to determine the elemental composition of materials. XRF analyzers determine the chemistry of a sample by measuring the fluorescent (or secondary) X-ray emitted from a sample when it is excited by a primary X-ray source. Each of the elements present in a sample produces a set of characteristic fluorescent X-rays (“a fingerprint”) that is unique for that specific element, which is why XRF spectroscopy is an excellent technology for qualitative and quantitative analysis of material composition.

5. Results of examination

5.1. Microstructure of test samples

The typical optical microstructure of NiTi1, NiTi2 and CuAlNi are shown in the Figs. 7a – 7c in order to view some details of the microstructure by using 50, 100, 200, 500 and 1000.

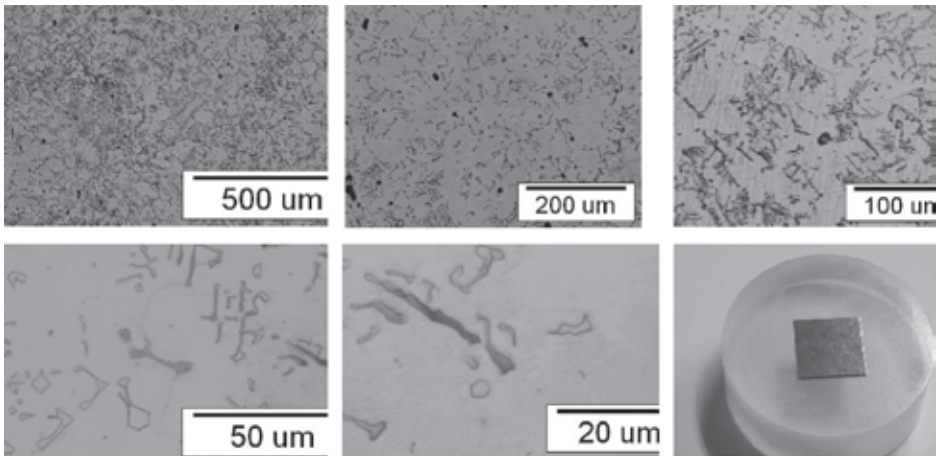


Figure 7a: NiTi 1 as cast – optical microstructure with the initial sample

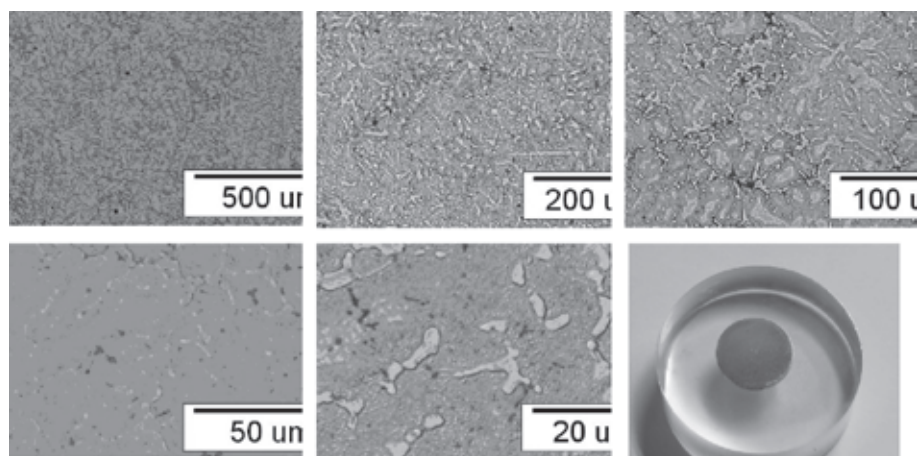


Figure 7b: NiTi 2 - CC – optical microstructure with the initial sample

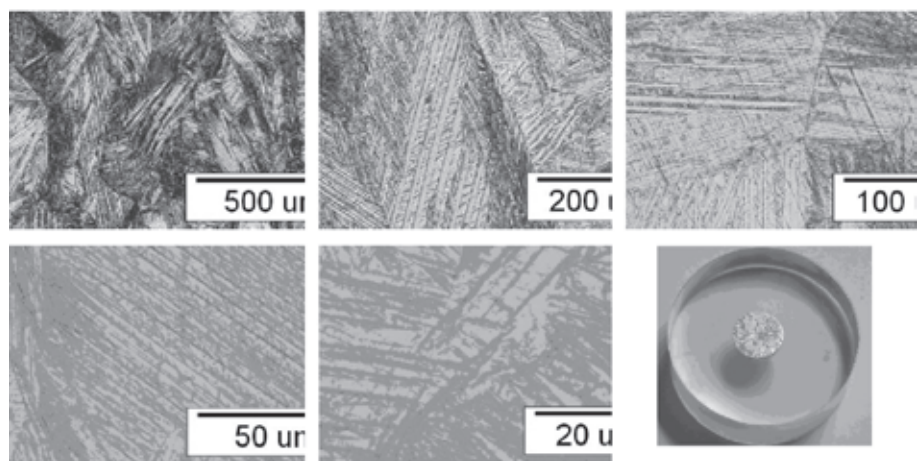


Figure 7c: CuAlNi 3 - CC – optical microstructure with the initial sample

NiTi microstructure is fine-grained, with the presence of small martensitic lamellae clearly visible in Figs. 7a and 7b (about 20 μm in length). On the other hand, CuAlNi microstructure has a coarser granular characteristic, with the presence of larger martensitic lamellae (about 200 μm in length) – as presented in Fig 7c.

5.2. Macro and micro hardness results of test sample

Figs. 8a-8c present the locations of hardness measurements on individual samples. Tables 3a and 3b show the results of microhardness HV5 and hardness HV50 on the

basis of 8 chosen positions with all statistics' data: Average, minimum, maximum and Standard Deviation.

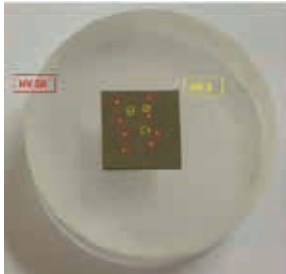


Figure 8a: Hardness measurement location - NiTi1

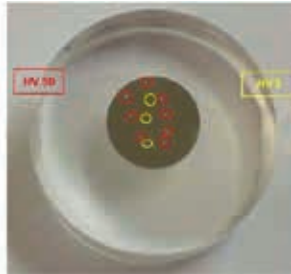


Figure 8b: Hardness measurement location - NiTi2

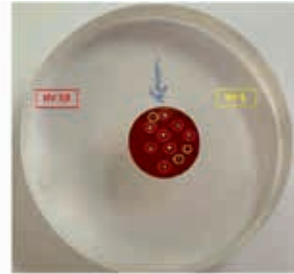


Figure 8c: Hardness measurement location - CuAlNi 3

Table 3a.: Micro-hardness results HV5

	NiTi 1	NiTi 2	CuAlNi 3
Average	275,00	630,00	279,67
Min	268	613	260
Max.	280	644	299
STDV	6,24	15,72	19,50

Table 3b: Hardness results HV50

	NiTi 1	NiTi 2	CuAlNi 3
Average	317,13	623,75	253,00
Min	289	586	229
Max.	357	644	266
STDV	22,89	20,32	12,43

The results revealed that the hardnesses HV5 and HV59 were the highest in the NiTi 2-CC sample (2 \times), which can be attributed to the new manufacturing technology-CC.

5.3. ICP Analyses results

ICP Analyses results for samples are shown in Table 4.

Table 4: ICP Analyses results for all samples

	% Ni	% Ti	% Fe	% Al	% Cu
NiTi 1	55,4	44,6			
NiTi 2	62,6	35,9	1,4		
CuAlNi 3	3,9		0,03	12,0	base

The analysis of NiTi 2 showed a content of element (Fe) that was not present in the raw materials. This is due to dissolution during the fabrication process (screw at CC).

5.4. XRF Analyses results

XRF Analyses results of test samples are shown in Table 5, where, for each sample, NiTi1, NiTi2 and CuAlNi3 represent the range between minimum and maximum values.

Table 5: XRF Analyses results for all samples

	% Ni	% Ti	% Fe	% Al	% Cu
NiTi 1	55,2 - 55,5	44,4 - 44,8			
NiTi 2	62,5-62,6	35,9	1,4		
CuAlNi 3	4,4			9,4 – 9,6	base

Also, the results of XRF analysis are consistent with the previous ICP. Based on this study, including the preparation of samples, testing basic properties (chemical composition, hardness) and microstructure, we laid the groundwork for further research for these SMAs, with a view to how corrosion processes affect their properties by changing the microstructure, chemical composition, and hardness. This will be the basis for transferring this knowledge to shipbuilding.

6. Conclusions

The study investigated the microstructures of NiTi alloys with a chemical composition of 50 at.% Ni and 50 at.% Ti using classical melting and CC. Both were compared with a CuAlNi rod, also manufactured by CC. The experiments performed resulted in the following conclusions:

1. The microstructure depends strongly on the manufacturing process and on the chemical composition. Both NiTi microstructures were finer grained, while, contrarily, CuAlNi is more granular.

2. The process of CC production in the form of a rod was demonstrated as one good option, because it gave high hardness of the produced NiTi rod.

3. In determining the chemical composition, several methods need to be used (ICP, XRF) to identify “inappropriate” elements. The presence of Fe was determined in NiTi 2. This may interfere with the use of this alloy for further processing operations necessary for shipbuilding.

Acknowledgement:

This paper is a result within the Eureka Project PROCHA-SMA, which was realised by the Faculty of Stomatology in Belgrade Serbia, Zlatarna Celje d.o.o. Serbia,

and the Faculty of Maritime Studies, Kotor, University of Montenegro, and the Faculty of Mechanical Engineering, Maribor, Slovenia – as a subcontractor.

Funding:

This research was funded by the BILATERAL PROJECT BI-ME/18-20-024 (2019-2020) Slovenia – Montenegro and EUREKA PROGRAM PROCHA-SMA funded by Ministry of Science of the Republic of Montenegro.

References:

1. Dye, T. E.,(1990), An Experimental Investigation of the Behavior of Nitinol, Master's Thesis, Department of Mechanical Engineering, Virginia Polytechnic Institute and State University
2. Weimin Huang, Shape Memory Alloys and their Application Disertation, University of Cambridge Department of Engineering, to Actuators for Deployable Structures, 1998.
3. EUROPEAN PATENT APPLICATION, EP 3 290 768 A1, Published in accordance with Art. 153(4) EPC, 2016.
4. J.A. Bezjak, The shape memory effect in systems of Cu based alloys, *Int. J. Innovative Res. Sci. Eng. Technol.* 2 (2) (2013) 485–492.
5. J.M. Jani, M. Leary, A. Subic, M.A. Gibson, A review of shape memory alloy research, applications and opportunities, *J. Mater. Des.* 56 (2014) 1078–1113.
6. M. Mishra, A.A. Ravindra, A comparison of conventional and iron based shape memory alloys and their potential in structural applications, *Int. J. Struct. Civ. Eng. Res.* 3 (4) (2014).
7. R. Amini, S.M. Mousavizad, H. Abdollahpour, M. Ghaffari, M. Alizadeh, A.K. Okyay, Structural and microstructural phase evolution during mechanosynthesis of nanocrystalline/amorphous CuAlMn alloy powders, *Adv. Powder Technol.* 24 (2013) 1048–1053.
8. Kenneth Kanayo Alaneme, Eloho Anita Okotete, Reconciling viability and cost-effective shape memory alloy options – A review of copper and iron based shape memory metallic systems, *Engineering Science and Technology, an International Journal* 19 (2016) 1582–1592
9. Jose San Juan, Applications of Shape Memory Alloys to the Transport Industry, International Congress on Innovative Solutions for the Advancement of the Transport Industry, At San Sebastian, Spain, October 2006.
10. Funakubo, H.(1987), Shape Memory Alloys, Gordon and Breach Science Publishers.
11. T. Lenau "Shape Memory Applications Inc.," Nitinol Devices & Components Inc. 2003. Available: <http://www.designinsite.dk/htmsider/m0173.html>.
12. TERNIK, Primož, ZADRAVEC, Matej, SVETEC, Milan, RUDOLF, Rebeka. Numerical analysis of the rapid solidification process of NiTi binary alloy. *Acta physica Polonica.A.* [Print ed.]. July 2015, vol. 128, no. 1, str. 43-47. ISSN 0587-4246. DOI: [10.12693/APhysPolA.128.43](https://doi.org/10.12693/APhysPolA.128.43).
13. STAMBOLIĆ, Aleš, JENKO, Monika, KOCIJAN, Aleksandra, ŽUŽEK, Borut, DROBNE, Damjana, RUDOLF, Rebeka. Determination of mechanical and functional properties by continuous vertical cast NiTi rod. *Materiali in tehnologije*. [Tiskana izd.]. sep.-okt. 2018, letn. 52, št. 5, str. 521-527, ilustr. ISSN 1580-2949. <http://mit.imt.si/Revija/izvodi/mit185/stambolic.pdf>, DOI: [10.17222/mit.2018.030](https://doi.org/10.17222/mit.2018.030).
14. TERNIK, Primož, ZADRAVEC, Matej, RUDOLF, Rebeka. Numerical analysis of the NiTi solidification process influence of thermal conductivity. *Science of sintering: the periodical of the International Institute for the Science of Sintering*. Jan-Mar. 2017, vol. 49, no. 1, str. 39-49. ISSN 0350-820X. DOI: [10.2298/SOS1701039T](https://doi.org/10.2298/SOS1701039T).
15. STAMBOLIĆ, Aleš, ANŽEL, Ivan, LOJEN, Gorazd, KOCIJAN, Aleksandra, JENKO, Monika, RUDOLF, Rebeka. Continuous vertical casting of a NiTi alloy. *Materiali in tehnologije*. [Tiskana izd.]. 2016, letn. 50, št. 6, str. 981-988. ISSN 1580-2949. DOI: [10.17222/mit.2016.111](https://doi.org/10.17222/mit.2016.111).

